HHS Public Access

Author manuscript

Dev Biol. Author manuscript; available in PMC 2024 November 01.

Published in final edited form as:

Dev Biol. 2024 November ; 515: 67–78. doi:10.1016/j.ydbio.2024.06.021.

Planarian LDB and SSDP proteins scaffold transcriptional complexes for regeneration and patterning

Taylor Medlock-Lanier[a,1], **Kendall B. Clay**[b,1], **Rachel H. Roberts-Galbraith**[a,*]

[a]Department of Cellular Biology, University of Georgia, Athens, GA, USA

[b]Neuroscience Program, University of Georgia, Athens, GA, USA

Abstract

Sequence-specific transcription factors often function as components of large regulatory complexes. LIM-domain binding protein (LDB) and single-stranded DNA-binding protein (SSDP) function as core scaffolds of transcriptional complexes in animals and plants. Little is known about potential partners and functions for LDB/SSDP complexes in the context of tissue regeneration. In this work, we find that planarian LDB1 and SSDP2 promote tissue regeneration, with a particular function in anterior regeneration and mediolateral polarity reestablishment. We find that LDB1 and SSDP2 interact with one another and with characterized planarian LIM-HD proteins Arrowhead, Islet1, and Lhx1/5–1. We also show that *SSDP2* and *LDB1* function with *islet1* in polarity reestablishment and with *lhx1/5–1* in serotonergic neuron maturation. Finally, we find new roles for LDB1 and SSDP2 in regulating gene expression in the planarian intestine and parenchyma; these functions are likely LIM-HD-independent. Together, our work provides insight into LDB/SSDP complexes in a highly regenerative organism. Further, our work provides a strong starting point for identifying and characterizing potential binding partners of LDB1 and SSDP2 and for exploring roles for these proteins in diverse aspects of planarian physiology.

Keywords

Planarian; Schmidtea; LDB; SSDP; Transcription factor; Gene Expression; Regeneration; Flatworm

1. Introduction

Dynamic gene expression drives consequential changes in cellular behavior during development and regeneration. Though DNA-binding transcription factors are sometimes

*Corresponding author. robertsgalbraith@uga.edu (R.H. Roberts-Galbraith).
[1]Authors contributed equally.

Appendix A. Supplementary data

Supplementary data to this article can be found online at https://doi.org/10.1016/j.ydbio.2024.06.021.

CRediT authorship contribution statement

Taylor Medlock-Lanier: Writing – review & editing, Visualization, Methodology, Investigation, Formal analysis, Data curation. **Kendall B. Clay:** Writing – review & editing, Visualization, Validation, Methodology, Investigation, Formal analysis, Data curation. **Rachel H. Roberts-Galbraith:** Writing – review & editing, Writing – original draft, Visualization, Validation, Supervision, Resources, Methodology, Investigation, Funding acquisition, Formal analysis, Data curation, Conceptualization.

considered in isolation, most such factors function *in vivo* in modular transcriptional complexes that bring together numerous gene regulatory proteins to elicit changes in chromatin architecture and transcriptional outcome. LIM-domain binding protein (LDB)—also known as CLIM, NLI, and CHIP—scaffolds transcriptional complexes with the help of single-stranded DNA-binding protein (SSDP) (Chen et al., 2002; van Meyel et al., 2003). LDB and SSDP-scaffolded complexes are ancient, present in diverse animals, and are related to similar scaffolding proteins (SEUSS/LEUNIG) that work together to organize gene regulatory complexes in plants (Franks et al., 2002; Sridhar et al., 2004; van Meyel et al., 2003).

As core transcriptional regulatory factors in gene expression across broad cell types in animals, LDB and SSDP orthologs play diverse roles in development, particularly in formation of the head and brain (Matthews and Visvader, 2003). *Drosophila Chip* was identified in a genetic screen as a regulator of wing morphology (Morcillo et al., 1996, 1997), and *Drosophila SSDP* is essential, with mutants lacking maternal and zygotic *SSDP* dying during larval development (Chen et al., 2002). *C. elegans SAM-10* (ortholog of *SSDP*) and *ldb-1* promote normal gene expression in neurons during maturation, modulating synapse and neurite formation (Cassata et al., 2000; Zheng et al., 2011). Zebrafish *SSDP* and *CLIM/LDB* paralogs function in neural patterning, eye formation, and sensory axon formation (Becker et al., 2002; Zhong et al., 2011). Mice lacking *ssdp1* develop with aberrant head morphogenesis; the initial mouse mutant of *ssdp1* was named *headshrinker* (Nishioka et al., 2005) and a proline-rich region within SSDP1 is important for head development (Enkhmandakh et al., 2006). Mice lacking LDB1 also develop with severe anterior truncations and defects in head development, as well as other pleiotropic phenotypes including heart defects and patterning problems (Mukhopadhyay et al., 2003), while murine LDB2 plays overlapping *and* unique roles in neural development (Gueta et al., 2016; Leone et al., 2017). Finally, LDB proteins can function in chromatin looping and recruitment of complexes to modify chromatin (Caputo et al., 2015; Krivega et al., 2014; Lee et al., 2016; Magli et al., 2019).

In animals, LDB/SSDP complexes often include LIM-homeodomain proteins and other sequence-specific DNA-binding transcription factors that direct the complex to specific regions of the genome (Matthews and Visvader, 2003) (Fig. 1A). LDB itself can function as a dimer or trimer, resulting in the potential bridging of two transcription factors together to form homo- or hetero-multimeric DNA-binding structures (Cross et al., 2010; Jurata et al., 1998; Wang et al., 2020). LDB complexes are best known for including LIM-HD proteins (Agulnick et al., 1996; Hobert and Westphal, 2000; Morcillo et al., 1997; van Meyel et al., 2003; Yasuoka and Taira, 2021). For example, murine Lim1 plays a critical role in head organization in development (Shawlot and Behringer, 1995), similar to functions of mouse LDB1 and SSDP. And murine Lhx2 cooperates with LDB1 for a narrower role during several neurodevelopmental processes, including regionalization of the hippocampus, development of olfactory neurons, and regulation of neurogenic vs. gliogenic choices in the retina (de Melo et al., 2018; Kinare et al., 2020; Monahan et al., 2019). Alternatively, LDB/SSDP complexes can also include transcriptional regulators that do *not* possess LIM domains. Additional LDB/SSDP-associated transcription factor proteins have been most thoroughly documented in *Drosophila*, where they include Pygopus, Bicoid,

Pannier, Groucho, and Ftz (Bronstein et al., 2010; Fiedler et al., 2015; Torigoi et al., 2000). Cooperation between LDB, SSDP, and transcription factors leads to varied outcomes.

SSDP and LDB homologs regulate head organization and neural development during embryogenesis, but few studies have explored potential roles for these core regulators during regeneration. We opted to explore potential functions of LDB, SSDP, and associated transcription factors in regeneration using planarian flatworms of the species *Schmidtea mediterranea*. Planarians complete whole-body regeneration from tiny fragments of starting tissue using adult, pluripotent stem cells (for review, see (Ivankovic et al., 2019)). During regeneration, planarians reestablish diverse cell types in organs that include muscle, a brain, protonephridia, and a muscular feeding organ called the pharynx (for review, see (Roberts-Galbraith and Newmark, 2015)). Due to their unique biology, planarians are outstanding model organisms with which to discover genetic mechanisms that regulate regeneration and stem cell biology. Planarian SSDP and LDB homologs have not been characterized, but LIM-homeodomain proteins have been described. Planarian *islet1* plays roles in reestablishment of anterior, posterior, and midline polarity (Hayashi et al., 2011; Marz et al., 2013). *lhx1/5–1* directs maturation of serotonergic neurons in the central and peripheral nervous system of the planarian (Currie and Pearson, 2013). And an *arrowhead* homolog is required for reestablishment of medial brain structures, including the anterior commissure, through creation of neurons that serve as guidepost cells (Roberts-Galbraith et al., 2016; Scimone et al., 2020). Recently, the full LIM-HD complement was characterized, with new roles for *lhx1/5–2* and *lhx2/9–1* in intestinal cell types being described (Molina et al., 2023).

Here, we identify and characterize roles for planarian LDB and SSDP homologs in the context of regeneration. We find that LDB1 and SSDP2 are required for proper regeneration, playing important roles in reestablishment of polarity. Using yeast two-hybrid assays, we show that LDB1 interacts with itself, with SSDP2, and with LIM-HD proteins Islet1, Lhx1/5–1, and Arrowhead. We further show that LDB1 and SSDP2 cooperate with binding partners Islet1 and Lhx1/5–1 in polarity reestablishment and serotonergic maturation, respectively. Broadening our study, we confirm the complement of genes that encode LIM-homeodomain proteins and identify related LIM-only domain proteins in planarians. Finally, to begin the process of discovering potential targets of SSDP2-containing complexes, we performed RNAi and RNA-sequencing to identify dozens of genes that depend on SSDP2 for proper expression. We conclude that planarian SSDP2 and LDB1 play key roles in regulating gene expression during planarian regeneration and homeostasis—both by cooperating with known LIM-HD partners and likely by partnering with other transcriptional regulators. Our work provides an important foundation for exploring the shared and unique roles of conserved LDB/SSDP complexes in the context of robust tissue regeneration.

2. Results and discussion

2.1. Planarian LDB1 and SSDP2 are required for blastema size and organization

To identify planarian LDB and SSDP homologs, we searched available transcriptomes (Brandl et al., 2016; Rozanski et al., 2019) and found two homologs each of *LDB* and *SSDP*

(Supp. Tables 1 and 2). We examined the expression patterns of planarian homologs and determined that *LDB1*, *LDB2*, *SSDP1*, and *SSDP2* have nearly ubiquitous expression with some potential enrichment in the planarian brain (Fig. 1B). Wide-ranging expression was also indicated in published single-cell sequencing atlases, with some specific enrichment of *LDB1* in subsets of *cathepsin*$^+$ cell types (Supp. Tables 1 and 2 (Fincher et al., 2018; Plass et al., 2018)). We also note that both *LDB1* and *SSDP2* were significantly upregulated at 36 h and 72 h post-amputation in our prior gene expression analysis (Supp. Fig. 1A (Roberts-Galbraith et al., 2016)).

Next, we investigated whether planarian LDB and SSDP homologs play roles in regeneration. We knocked down *LDB1*, *LDB2*, *SSDP1*, or *SSDP2*, amputated prepharyngeally, and allowed heads to regenerate for 6 days. We did not note any regeneration defects after *LDB2(RNAi)* or *SSDP1(RNAi)*. However, *LDB1(RNAi)* and *SSDP2(RNAi)* animals exhibited slower movement and regenerated with pointy head blastemas and cyclopia (Fig. 1C). We also repeated RNAi targeting each homolog, amputated heads, and examined brain organization at 6 days post-amputation (dpa) via *in situ* hybridization (ISH) with a *choline acetyltransferase* (*ChAT*) riboprobe (Nishimura et al., 2010). We found that brain regeneration proceeded normally after *LDB2(RNAi)* or *SSDP1 (RNAi)*. However, *LDB1(RNAi)* and *SSDP2(RNAi)* animals regenerated with significantly smaller brains that were fused at the midline (Fig. 1D and E). We validated specificity of the knockdowns to confirm that RNAi of one paralog did not impact the other, using reverse transcription and quantitative PCR (RT-qPCR, Supp. Figs. 1B–E). We also validated knockdown efficiency for all targets, observing significant knockdown for all targets and strong knockdowns of all targets except *LDB2,* for which we note that mRNA is present at very low levels in asexual animals compared to sexual animals (Supp. Figs. 1B–E (Davies et al., 2017)).

We also asked whether *LDB* and *SSDP* homologs cooperate with one another. We found that double knockdown of *SSDP1* and *SSDP2* did not strengthen the brain size or cyclopia phenotype beyond what we saw with *SSDP2(RNAi)* alone (Supp. Figs. 1F–H). The phenotype of *LDB1* (RNAi) *LDB2*(RNAi) animals was also similar to *LDB1*(RNAi) alone (Supp. Figs. 1F–H). We also saw no enhancement of phenotype when we combined *SSDP2*(RNAi) and *LDB1*(RNAi), potentially supporting our argument that these proteins work in the same processes and/or pathway (Supp. Figs. 1F–H). We do note that phenotypes were less penetrant in this paradigm, potentially due to dilution of the dsRNA. Taken together, we conclude that planarian LDB1 and SSDP2 are important for head regeneration, just as SSDP and LDB homologs are important for head development in mice (Mukhopadhyay et al., 2003; Nishioka et al., 2005). Given that we did not see strong phenotypes after *LDB2*(RNAi) or *SSDP1*(RNAi) in our analyses, we opted to focus on LDB1 and SSDP2 for the remainder of our studies.

2.2. Smed-LDB1 interacts with SSDP2 and LIM-HD binding partners

In other animals, LDB homologs scaffold protein complexes and bind to SSDP and LIM-HD proteins to regulate transcription (Fig. 1A (Matthews and Visvader, 2003)). To test whether planarian LDB1 binds similarly to SSDP and LIM-HD proteins, we turned to

yeast two-hybrid analysis. We decided to focus on the most well-characterized planarian LIM-HD proteins: Lhx1/5–1, Islet1, and Arrowhead (Currie and Pearson, 2013; Hayashi et al., 2011; Marz et al., 2013; Roberts-Galbraith et al., 2016; Scimone et al., 2020). We cloned full-length (FL) versions of each gene into yeast two-hybrid vectors to create fusions of planarian proteins with either the DNA-binding domain (BD, Bait) or the activation domain of GAL4 (AD, Prey) (Chien et al., 1991). We also cloned short (Sh) versions of each gene that included only the domains relevant for known protein-protein interactions (Fig. 2A). For LDB1, we cloned the dimerization domain and LIM-binding domain. For SSDP2, we cloned the conserved N-terminal domain. We cloned the N-termini of Islet1, Lhx1/5–1, and Arrowhead (Ah), including both LIM domains for each LIM-HD protein.

In this yeast two-hybrid system, pairs of plasmids are transformed into an auxotrophic strain of *Saccharomyces cerevisiae.* Interaction between bait and prey plasmids enables activation of gene expression to allow growth on drop-out media lacking histidine and adenine supplements. With this assay, we determined that full-length planarian LDB1 interacted with planarian SSDP2, Arrowhead, Lhx1/5–1, and Islet1 (Fig. 2B, Supp. Fig. 2A). We did not see evidence of LDB1 self-interaction using full-length protein, contrary to studies of LDB in other organisms. We were only able to establish binding of LDB1 to partners using LDB1 as bait, due to transactivation of planarian SSDP2, Islet1, and Lhx1/5–1 when fused with the DNA-binding domain (BD, bait) (Fig. 2B, grey boxes; Supp. Fig. 2A). This experimental complication suggests that full-length SSDP2, Islet1, and Lhx1/5–1 can directly recruit *S. cerevisiae* proteins to promote transcription.

We confirmed interactions and narrowed interaction domains using short (“Sh”) constructs. We found that the conserved interior of planarian LDB1 interacts with the conserved N-terminus of SSDP2 (Fig. 2C, Supp. Fig. 2B). We also found that conserved LDB1 domains interact with the LIM domains of Arrowhead, Islet1, and Lhx1/5–1 (Fig. 2C, Supp. Fig. 2B). We additionally detected some interaction of the short construct of LDB1 with itself in this assay (Fig. 2C, Supp. Fig. 2B), which implies that planarian LDB1 does indeed self-interact. We did not observe transactivation of any short construct, which indicates that the excluded regions of SSDP2 and LIM-HD proteins are responsible for transactivation in this system.

For proposed complex members to cooperate *in vivo*, they must be present in the same cells. We thus turned to double fluorescent *in situ* hybridization (dFISH) to determine whether mRNAs that encode LDB1 were present in the same cells as *SSDP2*, *arrowhead*, *islet-1*, and *lhx1/5*-1 mRNAs. We confirmed that *LDB1* was expressed very broadly in the animal using this method. Indeed, we did observe that cells positive for *SSDP2*, *arrowhead*, *islet-1*, and *lhx1/5*-1 mRNAs also contained puncta of *LDB1* transcript (Fig. 2D).

Through our experiments, we showed that planarian LDB1 and SSDP2 interact similarly to their homologs in other animals (Fig. 1A). Further, LDB1 can interact with the LIM domains of planarian Islet1, Lhx1/5–1, and Arrowhead. Smed-LDB1 also self-interacts, albeit weakly in this assay. These protein-protein interactions, along with coexpression, demonstrate potentially conserved organization and cooperative function within planarian LDB1/SSDP2 complexes.

2.3. LDB1 and SSDP2 cooperate with LIM-HD proteins Islet1 and Lhx1/5–1

Based on our determination that planarian LDB1 can bind to Arrowhead, Islet1, and Lhx1/5–1, we next sought to test whether planarian LDB1 and SSDP2 cooperate with these LIM-HD proteins. Lhx1/5–1 is expressed in cells throughout the central and peripheral nervous system and promotes maturation of serotonergic neurons (Fig. 3A (Currie and Pearson, 2013)). Knockdown of *lhx1/5–1* reduces expression of *tryptophan hydroxylase* (*TPH*), a marker of peripheral serotonergic neurons, without affecting TPH^{+} cells in the eyes (Fig. 3B, inset (Currie and Pearson, 2013; Nishimura et al., 2007)). To assess whether *LDB1* or *SSDP2* is required for the function of *lhx1/5–1* in serotonergic neurons, we performed RNAi and examined *TPH* expression (Fig. 3C). We found that expression of *TPH* in the peripheral nervous system was reduced after *LDB1(RNAi)* or *SSDP2(RNAi)* (Fig. 3C, insets). Peripharyngeal and eyespot expression were unchanged. We also detected cyclopia using the *TPH* marker that was not present after *lhx1/5–1(RNAi)* but was present after *islet1(RNAi),* as has been previously reported (Fig. 3B and C (Marz et al., 2013)). We also examined the impact of *LDB1*(RNAi) and *SSDP2*(RNAi) on *islet1* and *lhx1/5–1* transcript abundance, noting no change after *LDB1*(RNAi) and only a slight decrease in *islet1* mRNA after *SSDP2*(RNAi) (Supp. Figs. 3A–B). We conclude that LDB1 and SSDP2 overlap functionally with Lhx1/5–1 to promote gene expression and maturation in peripheral serotonergic neurons, supporting the idea that these proteins work in a transcriptional complex in this process.

Previous research indicated that planarian *islet1* is expressed in anterior and posterior poles during regeneration (Fig. 3A (Hayashi et al., 2011; Marz et al., 2013)), and we find that both *SSDP2* and *islet* are expressed broadly in regenerating tissue (Supp. Fig. 3C). Knockdown of *islet1* leads to eye fusion at the midline, failure to reestablish anterior and posterior poles, and defective gene expression at the midline (Hayashi et al., 2011; Marz et al., 2013). Due to the superficial similarities of the *islet1(RNAi)*, *SSDP2(RNAi)*, and *LDB1(RNAi)* phenotypes, we next investigated whether *SSDP2* and *LDB1* are required for reestablishment of polarity. *islet1(RNAi)* leads to reduced *wnt1* expression in regenerating tails after posterior amputation (Fig. 3D (Hayashi et al., 2011; Marz et al., 2013)). Similarly, *SSDP2(RNAi)* or *LDB1(RNAi)* decreases *wnt1* expression in regenerating tails (Fig. 3D). We also found that *SSDP2(RNAi)* or *LDB1(RNAi)* reduces *sFRP-1* expression in regenerating heads (Fig. 3E). We conclude that SSDP2 and LDB1 likely cooperate with Islet1 in regeneration of pole structures.

RNAi targeting planarian *islet-1* also leads to mediolateral patterning defects, which are reflected in regeneration of cyclopic heads and reduced expression of *slit* (Fig. 3F (Marz et al., 2013)). We confirmed that *islet1(RNAi)* specifically reduced the dorsal expression domain of slit after head regeneration, with a posterior shift in dorsal slit expression (Fig. 3F, arrowhead). We next investigated whether knockdown of *SSDP2* or *LDB1* phenocopied *islet1(RNAi)* impacts on *slit* expression. Indeed, *SSDP2(RNAi)* or *LDB1(RNAi)* led to reduced dorsal *slit* expression domains in regenerating animals (Fig. 3F, arrowheads), though ventral *slit* expression was less affected. Based on these results, we expected that *islet1*, *SSDP2*, and *LDB1* might be important for lateral regeneration as well as anterior regeneration. We performed RNAi targeting *islet1*, *SSDP2*, or *LDB1* and completed sagittal

amputations along the midline of the planarian body (Fig. 3G). We killed and fixed animals 9 days post-amputation and completed ISH with our *ChAT* riboprobe to investigate regeneration of internal structures (Fig. 3H). After lateral regeneration, *SSDP2(RNAi)* or *LDB1(RNAi)* led to diminished lateral regeneration, significantly smaller regenerated brain lobes, and frequently undetectable regenerated ventral nerve cords (Fig. 3H and I, Supp. Figs. 3D–E). We conclude that planarian LDB1 and SSDP2 play roles in midline reestablishment and lateral regeneration. Our data support the idea that Islet1 is the relevant partner for the SSDP2/LDB1 transcriptional complex during lateral and head regeneration, indicating conservation of the complex but not the specific LIM-HD protein in this context. However, the increased severity of *LDB1(RNAi)* and *SSDP2 (RNAi)* phenotypes (Fig. 3H and I) could mean that other transcriptional complex partners are also involved.

To demonstrate specificity of the documented phenotypes, we finally asked whether *LDB1*, *SSDP2*, and associated LIM-HD transcription factors were generally important for regeneration, using a pharynx regeneration assay. Animals were amputated prepharygeally and head pieces were allowed to regenerate trunks and tails. We examined regenerated pharynges at day 13 post-amputation using ISH with the pharynx marker *laminin* (Adler et al., 2014; Zayas et al., 2005) and saw no differences in pharynx size (Supp. Fig. 3F). Similarly, we did not detect any impact of LDB1, SSDP2, or LIM-HD perturbation on stem cell abundance or specialization during regeneration (Supp. Figs. 3G–H). Our results indicate that the regeneration phenotypes seen after *ldb1(RNAi)* and *ssdp2(RNAi)* are likely to reflect specific roles in regeneration of polarity and reestablishment of specific tissue types, rather than a broad or non-specific impact on cellular physiology.

2.4. Identification of additional planarian LIM-HD- and LMO-encoding genes

To identify other partners in LDB1/SSDP2 complexes, we first explored LIM-HD proteins. In addition to prior characterization of *islet1*, *arrowhead*, and *lhx1/5–1* (Currie and Pearson, 2013; Hayashi et al., 2011; Marz et al., 2013; Roberts-Galbraith et al., 2016; Scimone et al., 2020), a few additional LIM-HD-encoding proteins have been identified. A second homolog of Islet, *islet2*, is expressed in the anterior pole within the planarian head (Li et al., 2019). *lhx2/9–1* (previously called *lhx2b*) is expressed in the planarian intestine and RNAi causes a reduction in goblet cells (Forsthoefel et al., 2020; Molina et al., 2023). *lhx2/9–3* (previously *lhx2/9-like*) and *lhx3/4* (previously *lhx3/4-like*) were both identified as transcription factor-encoding genes expressed in planarian stem cells (Scimone et al., 2014).

We searched available transcriptomes (Brandl et al., 2016; Rozanski et al., 2019) to reveal the full complement of LIM-HD- and LMO-encoding genes in *S. mediterranea*. We found that planarians express 13 genes that encode proteins with a pair of LIM domains and a homeodomain (i.e. LIM-HD proteins) (Supp. Table 3). A recent work also identified and characterized the same set of LIM-HD-encoding genes (Molina et al., 2023). Because LIM-only (LMO) proteins also interact with LDB proteins, we identified 3 planarian genes that encode proteins with LIM domains only that have homology to *LMO* genes like beadex, rhombotin, and *lmo4* (Supp. Table 3, Supp. Fig. 4). We also identified 41 transcripts that encode proteins with LIM domains but that do not clearly belong within LIM-HD or LMO groups (Supp. Table 3).

Next, we sought to characterize additional LIM-HD- and LMO-encoding transcripts by determining their expression patterns. Our ISH for published transcripts largely confirmed previous expression patterns, with the additional finding that *islet1* is broadly expressed outside the poles and is strongly expressed in the planarian brain (Fig. 4A (Molina et al., 2023)). We found that two LIM-HD-encoding genes, *lhx2/9–1* (previously called *lhx2b*) and *lhx1/5–2*, are expressed in the planarian intestine (Fig. 4A (Molina et al., 2023)). We noted one gene, *lmx1a/b-4*, expressed in the parenchyma, and we saw enriched expression of the majority of LIM-HD genes in subsets of cells in the planarian brain (Fig. 4A (Molina et al., 2023)). We found that the three LMO-encoding genes had enriched expression in neurons and, for *lmo1/3–2*, in additional cell types (Fig. 4B). We saw broad concordance between our ISH results and results from single-cell sequencing analyses (Supp. Table 3 (Fincher et al., 2018; Plass et al., 2018)), though our ISH experiments and those of our colleagues also revealed region-specific expression patterns for several genes that were not significantly enriched in single-cell analyses (Molina et al., 2023). Taken together, the tissue-specific expression patterns of LIM-HD and LMO genes offer hints to potential functions of these transcription factors and additional LDB/SSDP complexes in planarian neurobiology and regeneration. Further, neural expression of *islet1* indicates that there are likely to be additional important roles still to be discovered for known LIM-HD transcription factors.

2.5. Impacts of SSDP2(RNAi) on gene expression in planarians

Finally, we sought to perturb elements of the conserved LDB1/SSDP2 transcriptional complex for several reasons. First, we wished to uncover downstream impacts of their perturbation. Second, we hoped to discover new functions for the complex. Third, we wanted to explore whether additional SSDP2 functions were accomplished through LIM-HD-dependent or independent mechanisms. We performed *SSDP2(RNAi)* in triplicate (Fig. 5A) and used bulk RNA-sequencing to identify genes differentially expressed after knockdown. We confirmed that *SSDP2* itself was 3.5x downregulated in the samples (Supp. Tables 4–5). We identified 64 upregulated transcripts and 53 downregulated transcripts after *SSDP2(RNAi)* (fold change ≥1.5x, corrected $P \leq 0.05$; Fig. 5B–Supp. Tables 4–5). A large percentage of genes downregulated after *SSDP2(RNAi)* are expressed in the intestine, in parenchymal cell types, or in *cathepsin*$^+$ cell types (Supp. Tables 4–5, examples in Fig. 5C).

We cloned a subset of differentially expressed genes and examined their expression after *SSDP2(RNAi)*, *LDB1(RNAi)*, or RNAi targeting candidate *LIM-HD* genes, using the same paradigm we had used for our sequencing experiment (Fig. 5A). We confirmed that *prosaposin* (*dd_215*) is downregulated in both existing and regenerating tissue in both the intestine and the pharynx after *SSDP2(RNAi)* or *LDB1(RNAi)* (Fig. 5D). Surprisingly, knockdown of *lhx1/5–2* or *lhx2/9–1*—the two intestine-expressed LIM-HD genes—did not alter *prosaposin* expression in our experiment (Fig. 5D). We also examined the expression of two parenchymal-expressed genes, *dd_120* and *dd_240*, and found that their expression was decreased in *SSDP2(RNAi)* and *LDB1(RNAi)* animals in both new and existing tissue (Fig. 5E–H). We hypothesized that parenchymal roles for LDB1/SSDP2 could be accomplished through the function of a parenchyma-expressed LIM-HD-encoding gene, *lmx1a/b-4.* However, neither *dd_120* nor *dd_240* exhibited altered expression after *lmx1a/*

b-4(RNAi) (Fig. 5E–H). One caveat of the RNA-Seq experiment is that we used the entire regenerating animals for our analysis; this could bias our results toward highly expressed genes as well as genes like *dd_215*, *dd_120*, and *dd_*240 that showed changes in gene expression in non-regenerating tissues after *SSDP2(RNAi)*.

Taken together, our work shows that SSDP2 impacts gene expression in the intestine and parenchyma, in addition to roles that it plays with LIM-HD proteins. We further find that *LDB1(RNAi)* phenocopies *SSDP2 (RNAi)* impacts on intestinal and parenchymal gene expression, indicating that the two proteins cooperate in all contexts that we explored. However, we were not able to assign a LIM-HD-encoding protein partner for either intestinal or parenchymal roles, suggesting that additional, LIM-HD-independent LDB1/SSDP2 complexes are likely to exist.

2.6. Conclusions and future directions

In this work, we characterized planarian homologs of LDB and SSDP and discovered that LDB1 and SSDP2 play roles in organization and polarity of new tissue during regeneration. Our results provide evidence that core transcriptional scaffolds can be useful to target during regeneration to prioritize transcriptional regulators for further study. We show that LDB1 binds to SSDP2 and to LIM-HD proteins Arrowhead, Lhx1/5–1, and Islet1. We further demonstrate that LDB1 and SSDP2 are required for functions of Lhx1/5–1 and Islet1 in serotonergic neuron maturation and polarity, respectively. We identified the full complement of LIM-HD- and LMO-encoding genes in planarians, though additional work will be required to characterize planarian LMO proteins and other non-LIM-domain transcriptional partners of the SSDP2/LDB1 complex. Due to the expression of many LIM-HD and LMO genes in the planarian nervous system as well as roles for LDB1 and SSDP2 in head regeneration, we are particularly eager to discover roles for LDB1/SSDP2 and related factors in neuronal regeneration and function. Future work might also reveal the extent to which scaffolding proteins mediate specific gene expression outcomes in cell types like neurons where long transcripts can be common (McCoy and Fire, 2024) and where transcription factors cooperate to generate exquisite cellular diversity (reviewed in (Guillemot, 2007)). To find novel roles for the scaffolds, we identified genes differentially regulated after *SSDP2(RNAi)* and discovered novel roles for the transcriptional core proteins in gene expression in the intestine and parenchyma of the planarian body. We expect that future work will reveal specific DNA target sequences for LDB1/SSDP2 complexes in each tissue and in both regeneration and tissue homeostasis. Taken together, our work has uncovered conserved roles for LDB/SSDP complexes in head formation and provides a starting point for further exploration of these ancient transcriptional scaffolds in animal regeneration.

3. Materials and methods

3.1. Planarian care

We used asexually reproducing *S. mediterranea* (strain CIW4 (Newmark and Sánchez Alvarado, 2000)) for all experiments. Planarians were housed in Montjuïc salts (Cebrià and Newmark, 2005) at 18 °C in the dark. We fed animals organic beef liver puree (White Oak Pastures, Bluffton, GA) approximately once per week. Animals for *in situ* hybridization or

RNA interference (RNAi) were starved at least one week prior to experiments. We also used gentamicin sulfate (50 μg/mL final concentration, Gemini Bio-Products) to treat animals as needed and during all RNAi experiments.

3.2. Sequence identification and domain analysis

We identified homologs of SSDP and LDB families using TBLASTN searches of *S. mediterranea* transcriptomes (Brandl et al., 2016; Rozanski et al., 2019). We used both BLAST and domain search resources at Planmine (Brandl et al., 2016; Rozanski et al., 2019) to identify genes that encode LIM-domain proteins (LIM domain = IPR001781, PF00412). LIM-HD-encoding genes were classified and named as per (Molina et al., 2023).

Translated LMO proteins were subjected to phylogenetic analysis alongside homologs of LMO proteins and other LIM domain proteins from other animal species (Supp. Text 1). The analysis was performed on the Phylogeny.fr platform (Dereeper et al., 2008) using the following parameters. Alignment was completed using MUSCLE (v3.8.31) using default settings for highest accuracy. Ambiguous regions were removed with Gblocks (v0.91b) with the following curation parameters: minimum length of block after gap cleaning = 10; no gap positions allowed; all segments with 8 contiguous nonconserved positions were rejected; 85% was the minimum number of sequences for a flank position. The phylogenetic tree was constructed with PhyML (v3.1/3.0 aLRT) using maximum likelihood, a WAG substitution model (0.147 estimated proportion of invariant sites) and 4 gamma-distributed rate categories to account for rate heterogeneity. The gamma shape parameter was estimated from the data (1.457) and reliability for internal branches was assessed using an aLRT test (SH-like). Finally, the tree was rendered with Tree Dyn (v198.3) and branch support values are displayed in percentages.

3.3. Molecular biology methods

For *in situ* hybridization and RNA interference experiments, we cloned 500–800 bp fragments of each gene into pJC53.2 (Collins et al., 2010). Briefly, cDNA was prepared from planarians using an iSCRIPT kit (Bio-Rad) and primers shown in Supp. Table 6 were used to amplify fragments of each gene using Platinum Taq (Invitrogen). PCR amplicons were ligated into pJC53.2, which had been digested with *Eam*1105I, using standard ligation methods. Kanamycin was used to select trans-formants and sequencing was used to verify insert sequences and orientation (Azenta).

For yeast two-hybrid analysis, full length and short fragments of *LDB1*, *SSDP2*, *islet1*, *lhx1/5–1*, and *arrowhead* were amplified from cDNA with Phusion polymerase (New England Biosciences). Primers were designed to include restriction sites and are described in Supplemental Table 6. Amplicons were digested with restriction enzymes as follows: *Bam*HI and *Pst*I (*LDB1*, *arrowhead*, *islet1*); EcoRI/*Pst*I (*SSDP2*); or SmaI and *Bam*HI (*lhx1/5–1*). Digested fragments were inserted into digested pGAD424 and pGBT9 through standard molecular methods. Inserts were sequenced using primers described in Supp. Table 7.

To generate dsRNA and riboprobes, we amplified pJC53.2 inserts using a T7 primer (sequence in Supp. Table 7). PCR products were purified with a DNA clean and concentrator

kit (Zymo). We synthesized dsRNA as previously described (Chong et al., 2013; Rouhana et al., 2013). Riboprobes were generated from PCR products at 30 °C overnight using either Sp6 or T3 polymerase, depending on the orientation of the insert. We included digoxigenin-11-UTP (Roche), DNP-11-UTP (Per-kins-Elmer), or FITC-12-UTP (Roche) during riboprobe synthesis. Riboprobes were treated with DNase (Promega) and purified by ammonium acetate precipitation. Riboprobes and dsRNA concentrations were determined through band intensity after gel electrophoresis, which we have found to be more reliable than a spectrophotometer as only full-length products are quantified.

3.4. Yeast two-hybrid analysis

Saccharomyces cerevisiae strain PJ69–4 A was used for yeast two-hybrid analysis as previously described (James et al., 1996). Trans-formants were selected on agar plates made from dropout media (-Trp, -Leu). Interactions were evaluated on agar that was -His or -His -Ade (Clontech, now Takara Bio). Growth in the absence of either supplement indicates transcription from reconstituted GAL4 proteins. Empty vectors were used as negative controls. A pair of plasmids producing *Schizosaccharomyces pombe* Mob1 and Sid2 was used as a positive control (Hou et al., 2004; Salimova et al., 2000).

3.5. In situ hybridization

Whole and regenerating planarians were processed for *in situ* hybridization as described in (King and Newmark, 2013). Riboprobes produced as described above were detected using alkaline-phosphatase-conjugated anti-digoxigenin Fab fragments (1:2000, [Roche]). Colorimetric signals were generated using a development solution containing 5-Bromo-4-chloro-3-indolyl phosphate (BCIP, [Roche]) and nitro blue tetrazolium chloride (NBT, [Roche]). For fluorescent *in situ* hybridization, we also used a protocol from (King and Newmark, 2013). We used either anti-DIG-Peroxidase (Roche) at a concentration of 1:2000 or anti-DNP-HRP (Vector Labs) at a concentration of 1:1000 (Vector Labs). Fluorescent samples were stained with 4′,6-diamidino-2-phenylindole (DAPI, Sigma), washed, and mounted in VectaShield Antifade mounting medium (Vector Labs).

3.6. RNA interference

2–5 μg dsRNA generated as described above was combined with 30 μL of 4:1 liver:salts mix for each feeding. RNA feeding paradigms consisted of 3 feedings per experiment, with the first feeding on day 1, the second feeding on day 6, and the third feeding between days 10–12. Amputation occurred 5–7 days after the final feeding along prepharyngeal (anterior to the pharynx), postpharyngeal (posterior to the pharynx), or sagittal (down the midline) amputation planes. Animals were fixed and killed (or processed for RNA purification) 6 days post-amputation, with the exception being 74 h post-amputation for the posterior regeneration experiments (Fig. 3D), 9 days post-amputation for lateral regeneration experiments (Fig. 3G and H), and 15 days post-amputation for pharyngeal regeneration experiments (Supp. Fig. 3F). *dsRNA* matching *Aequorea green fluorescent protein* (*GFP*) was used as a negative control in RNAi experiments.

For double RNAi experiments, we acclimated 12 starved animals per sample to Petri dishes prior to experimentation. All dsRNA used was diluted to 500 ng/ul before mixing. Each

condition received 10 μg of total dsRNA per feeding (with 30 μL beef liver and 1 μL food dye), including 5 μg for each gene in the pair and *GFP* dsRNA used to make sure total dsRNA feeding was equivalent across conditions. Animals were allowed to eat for 2 h before being cleaned and transferred to new dishes with 20 μl of 50 mg/mL gentamycin sulfate (GeminiBio). Animals for double RNAi experiments were fed on day 0, day 5, day 9, amputated on day 16, and killed and fixed on day 23.

3.7. Microscopy

Animals that had been subjected to *in situ* hybridization were mounted in 80% glycerol or 1xPBS prior to imaging. Stained and live animals were imaged with either an Axiocam color camera mounted on a Zeiss Axio Zoom.V16 microscope or with a Leica DFC420 camera mounted on a Leica M205A stereomicroscope. Images of yeast strains (Supp. Fig. 2) were captured on an Apple iPhone 5. Fluorescent microscopy samples were imaged on a Zeiss LSM 880 confocal microscope using Zen Black 2.3 SPI software with an upright AXIO imager Z2. Samples were imaged with the 40x objective using an oil droplet on the coverslip. *LDB1*/*SSDP2* images were taken with a 2x zoom and *LDB1*/*lhx1/5–1* images were taken with a 1.5x zoom.

3.8. RNA sequencing and analysis

For each control and *SSDP2(RNAi)* samples, 4 plates of 10 worms were fed dsRNA as per the paradigm above. Animals were amputated prepharyngeally 5 days after the final feeding. 6 days post-amputation, animals for each sample were transferred to a 1.5 mL tube and salts were replaced with 250 μL TRIzol reagent (Invitrogen) before freezing on dry ice for storage at −80 °C. RNAs were purified from each sample as per the manufacturer's protocol, were DNAse treated (Promega), and were further cleaned with an RNA clean and concentrator kit (Zymo Research). RNAs were eluted 2x in 8 μL RNAse-free water. Three samples for each RNAi condition were submitted for quality analysis and library preparation with Illumina's TruSeq Stranded mRNAseq kit. Libraries were sequenced on a HiSeq 4000 platform (100 nt sequencing, using sequencing kit v.1). Fastq files were demultiplexed and adaptors were trimmed. We received between 37 million and 45 million reads per sample. RNA-seq reads have been deposited as BioProject PRJNA907760 (Accession: SRX18465766-SRX18465771).

Sequences were imported into CLC Genomics Workbench 8 (QIAgen) and were mapped to the dd_Smed_v6 transcriptome (Brandl et al., 2016; Rozanski et al., 2019) using "batch" mode and standard parameters. We then completed gene expression comparison (EDGE) and statistical analysis, with a filter cutoff of 3 counts and with FDR correction. We present data in Supp. Tables 4–5 with common and tagwise dispersion. For further analysis, we prioritized genes with $P < 0.05$ after FDR correction and with the highest fold changes.

3.9. Quantitative PCR

RNA was extracted from RNAi-treated animals and cDNA synthesis was completed as described above. Primers for qPCR were designed to capture regions of transcripts that do not overlap with dsRNA synthesis (Supp. Table 7). For each sample, three technical replicates of qPCR were completed; we also used three biological replicates for each

condition. *β-tubulin* mRNA was used to normalize overall mRNA abundance for all qPCR experiments. qPCR data were analyzed using GraphPad Prism 9. Statistical analyses were completed using an unpaired T-test (with Welch's correction when needed).

Supplementary Material

Refer to Web version on PubMed Central for supplementary material.

Acknowledgements

The authors thank Dr. Phillip Newmark and past members of the Newmark laboratory for their feedback on this project in its earliest stages. We thank current and past members of the Roberts-Galbraith laboratory for feedback and support during this project. We are grateful to Drs. M. Delores (Loli) Molina Jimenez and Francesc Cebrià for helpful discussion and for sharing their work on planarian LIM-HD genes. We are grateful to Dr. Alejandro Sánchez Alvarado and Shane Merryman, of the Stowers Institute for Medical Research, for providing *S. mediterranea* during our laboratory start-up and for sharing advice on planarian aquaculture. We thank Dr. Alvaro Hernandez and the staff of the Roy J. Carver Biotechnology Center (University of Illinois, Urbana-Champaign) for sequencing and experimental design advice for our RNA-sequencing experiments. We thank Sebastien Santini (CNRS/AMU IGS UMR7256) and the PACA Bioinfo platform for maintenance and availability of the phylogeny.fr website that we used to create our phylogeny. We thank Dr. Kathleen Gould (Vanderbilt University) for sharing yeast strains and plasmids used in yeast two-hybrid analysis. We also thank the farmers and staff of White Oak Pastures for raising healthy cattle and providing beef liver we use to feed our planarians (Bluffton, GA). This work was supported by funding from the McKnight Foundation (McKnight Scholars Award to RRG) and the National Institute for Neurological Disease and Stroke at the National Institutes of Health (1R01NS128096–01). KBC was supported by the National Institute of General Medical Sciences of the National Institute of Health under award number 1T32GM142623 and the National Institute of Neurological Disorders and Stroke of the National Institute of Health under project number 5R25NS107179–02. KBC was also supported by the University of Georgia Research Foundation and the ARCS Foundation.

Data availability

Data will be made available on request.

Abbreviations:

CLIM	co-factor of LIM domains
DNA	deoxyribonucleic acid
dpa	days post-amputation
ISH	*in situ* hybridization
LDB	LIM domain binding protein
LIM	LIN-11, Isl-1, and Mec3
LIM-HD	LIM homeodomain
LHX	LIM homeobox
LMO	LIM only
RNA	ribonucleic acid
SSDP	single-stranded DNA-binding protein

References

Adell T, Saló E, Boutros M, Bartscherer K, 2009. Smed-Evi/Wntless is required for beta-catenin-dependent and -independent processes during planarian regeneration. Development 136, 905–910. [PubMed: 19211673]

Adler CE, Seidel CW, McKinney SA, Sánchez Alvarado A, 2014. Selective amputation of the pharynx identifies a FoxA-dependent regeneration program in planaria. Elife 3, e02238.

Agulnick AD, Taira M, Breen JJ, Tanaka T, Dawid IB, Westphal H, 1996. Interactions of the LIM-domain-binding factor Ldb1 with LIM homeodomain proteins. Nature 384, 270–272. [PubMed: 8918878]

Balasubramanian MK, McCollum D, Chang L, Wong KC, Naqvi NI, He X, Sazer S, Gould KL, 1998. Isolation and characterization of new fission yeast cytokinesis mutants. Genetics 149, 1265–1275. [PubMed: 9649519]

Becker T, Ostendorff HP, Bossenz M, Schluter A, Becker CG, Peirano RI, Bach I, 2002. Multiple functions of LIM domain-binding CLIM/NLI/Ldb cofactors during zebrafish development. Mech. Dev. 117, 75–85. [PubMed: 12204249]

Brandl H, Moon H, Vila-Farre M, Liu SY, Henry I, Rink JC, 2016. PlanMine - a mineable resource of planarian biology and biodiversity. Nucleic Acids Res. 44, D764–D773. [PubMed: 26578570]

Bronstein R, Levkovitz L, Yosef N, Yanku M, Ruppin E, Sharan R, Westphal H, Oliver B, Segal D, 2010. Transcriptional regulation by CHIP/LDB complexes. PLoS Genet. 6, e1001063.

Caputo L, Witzel HR, Kolovos P, Cheedipudi S, Looso M, Mylona A, van IWF, Laugwitz KL, Evans SM, Braun T, et al. , 2015. The Isl1/Ldb1 complex Orchestrates genome-wide chromatin organization to instruct differentiation of Multipotent Cardiac progenitors. Cell Stem Cell 17, 287–299. [PubMed: 26321200]

Cassata G, Rohrig S, Kuhn F, Hauri HP, Baumeister R, Burglin TR, 2000. The Caenorhabditis elegans Ldb/NLI/Clim orthologue ldb-1 is required for neuronal function. Dev. Biol. 226, 45–56. [PubMed: 10993673]

Cebrià F, Guo T, Jopek J, Newmark PA, 2007. Regeneration and maintenance of the planarian midline is regulated by a *slit* orthologue. Dev. Biol. 307, 394–406. [PubMed: 17553481]

Cebrià F, Newmark PA, 2005. Planarian homologs of *netrin* and *netrin receptor* are required for proper regeneration of the central nervous system and the maintenance of nervous system architecture. Development 132, 3691–3703. [PubMed: 16033796]

Chen L, Segal D, Hukriede NA, Podtelejnikov AV, Bayarsaihan D, Kennison JA, Ogryzko VV, Dawid IB, Westphal H, 2002. Ssdp proteins interact with the LIM-domain-binding protein Ldb1 to regulate development. Proc Natl Acad Sci U S A 99, 14320–14325. [PubMed: 12381786]

Chien CT, Bartel PL, Sternglanz R, Fields S, 1991. The two-hybrid system: a method to identify and clone genes for proteins that interact with a protein of interest. Proc Natl Acad Sci U S A 88, 9578–9582. [PubMed: 1946372]

Chong T, Collins JJ 3rd, Brubacher JL, Zarkower D, Newmark PA, 2013. A sex-specific transcription factor controls male identity in a simultaneous hermaphrodite. Nat. Commun. 4, 1814. [PubMed: 23652002]

Collins JJ 3rd, Hou X, Romanova EV, Lambrus BG, Miller CM, Saberi A, Sweedler JV, Newmark PA, 2010. Genome-wide analyses reveal a role for peptide hormones in planarian germline development. PLoS Biol. 8, e1000509.

Cross AJ, Jeffries CM, Trewhella J, Matthews JM, 2010. LIM domain binding proteins 1 and 2 have different oligomeric states. Journal of molecular biology 399, 133–144. [PubMed: 20382157]

Currie KW, Pearson BJ, 2013. Transcription factors *lhx1/5–1* and *pitx* are required for the maintenance and regeneration of serotonergic neurons in planarians. Development 140, 3577–3588. [PubMed: 23903188]

Davies EL, Lei K, Seidel CW, Kroesen AE, McKinney SA, Guo L, Robb SM, Ross EJ, Gotting K, Alvarado AS, 2017. Embryonic origin of adult stem cells required for tissue homeostasis and regeneration. Elife 6.

de Melo J, Clark BS, Venkataraman A, Shiau F, Zibetti C, Blackshaw S, 2018. Ldb1- and Rnf12-dependent regulation of Lhx2 controls the relative balance between neurogenesis and gliogenesis in the retina. Development 145.

Dereeper A, Guignon V, Blanc G, Audic S, Buffet S, Chevenet F, Dufayard JF, Guindon S, Lefort V, Lescot M, et al. , 2008. Phylogeny.fr: robust phylogenetic analysis for the non-specialist. Nucleic Acids Res. 36, W465–W469. [PubMed: 18424797]

Enkhmandakh B, Makeyev AV, Bayarsaihan D, 2006. The role of the proline-rich domain of Ssdp1 in the modular architecture of the vertebrate head organizer. Proc Natl Acad Sci U S A 103, 11631–11636. [PubMed: 16864769]

Fiedler M, Graeb M, Mieszczanek J, Rutherford TJ, Johnson CM, Bienz M, 2015. An ancient Pygo-dependent Wnt enhanceosome integrated by Chip/LDB-SSDP. Elife 4.

Fincher CT, Wurtzel O, de Hoog T, Kravarik KM, Reddien PW, 2018. Cell type transcriptome atlas for the planarian *Schmidtea mediterranea*. Science 360.

Forsthoefel DJ, Cejda NI, Khan UW, Newmark PA, 2020. Cell-type diversity and regionalized gene expression in the planarian intestine. Elife 9.

Franks RG, Wang C, Levin JZ, Liu Z, 2002. SEUSS, a member of a novel family of plant regulatory proteins, represses floral homeotic gene expression with LEUNIG. Development 129, 253–263. [PubMed: 11782418]

Gueta K, David A, Cohen T, Menuchin-Lasowski Y, Nobel H, Narkis G, Li L, Love P, de Melo J, Blackshaw S, et al. , 2016. The stage-dependent roles of Ldb1 and functional redundancy with Ldb2 in mammalian retinogenesis. Development 143, 4182–4192. [PubMed: 27697904]

Guillemot F, 2007. Spatial and temporal specification of neural fates by transcription factor codes. Development 134, 3771–3780. [PubMed: 17898002]

Gurley KA, Rink JC, Sánchez Alvarado A, 2008. Beta-catenin defines head versus tail identity during planarian regeneration and homeostasis. Science 319, 323–327. [PubMed: 18063757]

Hayashi T, Motoishi M, Yazawa S, Itomi K, Tanegashima C, Nishimura O, Agata K, Tarui H, 2011. A LIM-homeobox gene is required for differentiation of Wnt-expressing cells at the posterior end of the planarian body. Development 138, 3679–3688. [PubMed: 21828095]

Hobert O, Westphal H, 2000. Functions of LIM-homeobox genes. Trends Genet. : TIG (Trends Genet.) 16, 75–83. [PubMed: 10652534]

Hou MC, Guertin DA, McCollum D, 2004. Initiation of cytokinesis is controlled through multiple modes of regulation of the Sid2p-Mob1p kinase complex. Mol. Cell Biol. 24, 3262–3276. [PubMed: 15060149]

Ivankovic M, Haneckova R, Thommen A, Grohme MA, Vila-Farre M, Werner S, Rink JC, 2019. Model systems for regeneration: planarians. Development 146.

James P, Halladay J, Craig EA, 1996. Genomic libraries and a host strain designed for highly efficient two-hybrid selection in yeast. Genetics 144, 1425–1436. [PubMed: 8978031]

Jurata LW, Pfaff SL, Gill GN, 1998. The nuclear LIM domain interactor NLI mediates homo- and heterodimerization of LIM domain transcription factors. J. Biol. Chem. 273, 3152–3157. [PubMed: 9452425]

Kinare V, Iyer A, Padmanabhan H, Godbole G, Khan T, Khatri Z, Maheshwari U, Muralidharan B, Tole S, 2020. An evolutionarily conserved Lhx2-Ldb1 interaction regulates the acquisition of hippocampal cell fate and regional identity. Development 147.

King RS, Newmark PA, 2013. In situ hybridization protocol for enhanced detection of gene expression in the planarian *Schmidtea mediterranea*. BMC Dev. Biol. 13, 8. [PubMed: 23497040]

Krivega I, Dale RK, Dean A, 2014. Role of LDB1 in the transition from chromatin looping to transcription activation. Genes & development 28, 1278–1290. [PubMed: 24874989]

Lee B, Lee S, Agulnick AD, Lee JW, Lee SK, 2016. Single-stranded DNA binding proteins are required for LIM complexes to induce transcriptionally active chromatin and specify spinal neuronal identities. Development 143, 1721–1731. [PubMed: 26965372]

Leone DP, Panagiotakos G, Heavner WE, Joshi P, Zhao Y, Westphal H, McConnell SK, 2017. Compensatory Actions of ldb adaptor proteins during Corticospinal motor neuron differentiation. Cerebr. Cortex 27, 1686–1699.

Li DJ, McMann CL, Reddien PW, 2019. Nuclear receptor NR4A is required for patterning at the ends of the planarian anterior-posterior axis. Elife 8.

Magli A, Baik J, Pota P, Cordero CO, Kwak IY, Garry DJ, Love PE, Dynlacht BD, Perlingeiro RCR, 2019. Pax3 cooperates with Ldb1 to direct local chromosome architecture during myogenic lineage specification. Nat. Commun. 10, 2316. [PubMed: 31127120]

Marz M, Seebeck F, Bartscherer K, 2013. A Pitx transcription factor controls the establishment and maintenance of the serotonergic lineage in planarians. Development 140, 4499–4509. [PubMed: 24131630]

Matthews JM, Visvader JE, 2003. LIM-domain-binding protein 1: a multifunctional cofactor that interacts with diverse proteins. EMBO Rep. 4, 1132–1137. [PubMed: 14647207]

McCoy MJ, Fire AZ, 2024. Parallel gene size and isoform expansion of ancient neuronal genes. Curr. Biol. 34, 1635–1645 e1633. [PubMed: 38460513]

Molina MD, Abduljabbar D, Guixeras A, Fraguas S, Cebria F, 2023. LIM-HD transcription factors control axial patterning and specify distinct neuronal and intestinal cell identities in planarians. Open Biol 13, 230327.

Monahan K, Horta A, Lomvardas S, 2019. LHX2- and LDB1-mediated trans interactions regulate olfactory receptor choice. Nature 565, 448–453. [PubMed: 30626972]

Morcillo P, Rosen C, Baylies MK, Dorsett D, 1997. Chip, a widely expressed chromosomal protein required for segmentation and activity of a remote wing margin enhancer in *Drosophila*. Genes & development 11, 2729–2740. [PubMed: 9334334]

Morcillo P, Rosen C, Dorsett D, 1996. Genes regulating the remote wing margin enhancer in the Drosophila cut locus. Genetics 144, 1143–1154. [PubMed: 8913756]

Mukhopadhyay M, Teufel A, Yamashita T, Agulnick AD, Chen L, Downs KM, Schindler A, Grinberg A, Huang SP, Dorward D, et al. , 2003. Functional ablation of the mouse Ldb1 gene results in severe patterning defects during gastrulation. Development 130, 495–505. [PubMed: 12490556]

Newmark PA, Sánchez Alvarado A, 2000. Bromodeoxyuridine specifically labels the regenerative stem cells of planarians. Dev. Biol. 220, 142–153. [PubMed: 10753506]

Nishimura K, Kitamura Y, Inoue T, Umesono Y, Yoshimoto K, Takeuchi K, Taniguchi T, Agata K, 2007. Identification and distribution of *tryptophan hydroxylase (TPH)*-positive neurons in the planarian *Dugesia japonica*. Neurosci. Res. 59, 101–106. [PubMed: 17624455]

Nishimura K, Kitamura Y, Taniguchi T, Agata K, 2010. Analysis of motor function modulated by cholinergic neurons in planarian Dugesia japonica. Neuroscience 168, 18–30. [PubMed: 20338223]

Nishioka N, Nagano S, Nakayama R, Kiyonari H, Ijiri T, Taniguchi K, Shawlot W, Hayashizaki Y, Westphal H, Behringer RR, et al. , 2005. Ssdp1 regulates head morphogenesis of mouse embryos by activating the Lim1-Ldb1 complex. Development 132, 2535–2546. [PubMed: 15857913]

Petersen CP, Reddien PW, 2008. *Smed-betacatenin-1* is required for anteroposterior blastema polarity in planarian regeneration. Science 319, 327–330. [PubMed: 18063755]

Plass M, Solana J, Wolf FA, Ayoub S, Misios A, Glazar P, Obermayer B, Theis FJ, Kocks C, Rajewsky N, 2018. Cell type atlas and lineage tree of a whole complex animal by single-cell transcriptomics. Science 360.

Roberts-Galbraith RH, Brubacher JL, Newmark PA, 2016. A functional genomics screen in planarians reveals regulators of whole-brain regeneration. Elife 5 (pii), e17002.

Roberts-Galbraith RH, Newmark PA, 2015. On the organ trail: insights into organ regeneration in the planarian. Curr. Opin. Genet. Dev. 32, 37–46. [PubMed: 25703843]

Rouhana L, Weiss JA, Forsthoefel DJ, Lee H, King RS, Inoue T, Shibata N, Agata K, Newmark PA, 2013. RNA interference by feeding *in vitro*-synthesized double-stranded RNA to planarians: Methodology and dynamics. Dev Dyn 242, C1.

Rozanski A, Moon H, Brandl H, Martin-Duran JM, Grohme MA, Huttner K, Bartscherer K, Henry I, Rink JC, 2019. PlanMine 3.0-improvements to a mineable resource of flatworm biology and biodiversity. Nucleic Acids Res. 47, D812–D820. [PubMed: 30496475]

Salimova E, Sohrmann M, Fournier N, Simanis V, 2000. The S. pombe orthologue of the S. cerevisiae mob1 gene is essential and functions in signalling the onset of septum formation. J. Cell Sci. 113 (Pt 10), 1695–1704. [PubMed: 10769201]

Scimone ML, Atabay KD, Fincher CT, Bonneau AR, Li DJ, Reddien PW, 2020. Muscle and neuronal guidepost-like cells facilitate planarian visual system regeneration. Science.

Scimone ML, Kravarik KM, Lapan SW, Reddien PW, 2014. Neoblast specialization in regeneration of the planarian *Schmidtea mediterranea*. Stem Cell Rep. 3, 339–352.

Shawlot W, Behringer RR, 1995. Requirement for Lim1 in head-organizer function. Nature 374, 425–430. [PubMed: 7700351]

Sridhar VV, Surendrarao A, Gonzalez D, Conlan RS, Liu Z, 2004. Transcriptional repression of target genes by LEUNIG and SEUSS, two interacting regulatory proteins for Arabidopsis flower development. Proc Natl Acad Sci U S A 101, 11494–11499. [PubMed: 15277686]

Torigoi E, Bennani-Baiti IM, Rosen C, Gonzalez K, Morcillo P, Ptashne M, Dorsett D, 2000. Chip interacts with diverse homeodomain proteins and potentiates bicoid activity in vivo. Proc Natl Acad Sci U S A 97, 2686–2691. [PubMed: 10688916]

van Meyel DJ, Thomas JB, Agulnick AD, 2003. Ssdp proteins bind to LIM-interacting co-factors and regulate the activity of LIM-homeodomain protein complexes in vivo. Development 130, 1915–1925. [PubMed: 12642495]

Wang H, Kim J, Wang Z, Yan XX, Dean A, Xu W, 2020. Crystal structure of human LDB1 in complex with SSBP2. Proc Natl Acad Sci U S A 117, 1042–1048. [PubMed: 31892537]

Yasuoka Y, Taira M, 2021. LIM homeodomain proteins and associated partners: then and now. Curr. Top. Dev. Biol. 145, 113–166. [PubMed: 34074528]

Zayas RM, Hernández A, Habermann B, Wang Y, Stary JM, Newmark PA, 2005. The planarian *Schmidtea mediterranea* as a model for epigenetic germ cell specification: analysis of ESTs from the hermaphroditic strain. Proc Natl Acad Sci U S A 102, 18491–18496. [PubMed: 16344473]

Zheng Q, Schaefer AM, Nonet ML, 2011. Regulation of C. elegans presynaptic differentiation and neurite branching via a novel signaling pathway initiated by SAM-10. Development 138, 87–96. [PubMed: 21115607]

Zhong Z, Ma H, Taniguchi-Ishigaki N, Nagarajan L, Becker CG, Bach I, Becker T, 2011. SSDP cofactors regulate neural patterning and differentiation of specific axonal projections. Dev. Biol. 349, 213–224. [PubMed: 21056553]

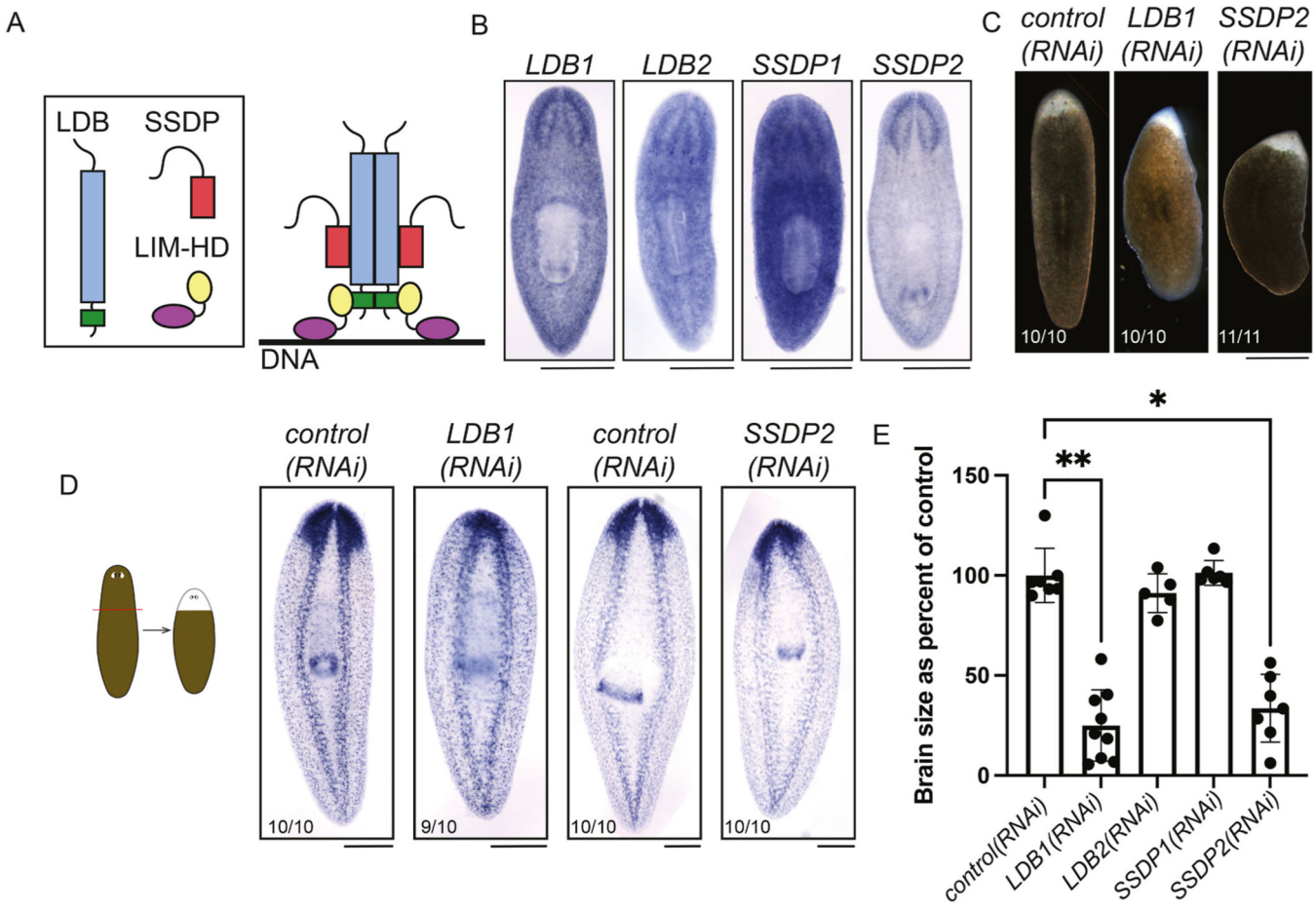

Fig. 1. Planarian SSDP and LDB homologs promote regeneration.

A) Diagram showing domain architecture in canonical LDB transcriptional complexes (Bronstein et al., 2010; Enkhmandakh et al., 2006). LDB = LIM Domain Binding protein; SSDP=Single-Stranded DNA Binding Protein; and LIM-HD = LIM-Homeodomain, where LIM is a region of homology first identified between Lin-11, Isl-1 and Mec-3. LDB proteins have a long dimerization domain (blue) and a LIM-binding domain (green). SSDP proteins have a conserved domain (red) and a long, unstructured region. LIM-HD proteins have a pair of LIM domains (yellow) and a homeodomain (purple). Complexes form to bind DNA and regulate gene expression. B) *in situ* hybridization showing expression patterns of planarian *LDB1*, *LDB2*, *SSDP1*, and *SSDP2*. All four genes are broadly expressed with some enrichment, particularly for *LDB1* and *SSDP2,* in the brain. C) Images of live planarians after RNAi, head amputation, and 6 days of regeneration. *control(RNAi)* animals have a rounded blastema with two eyespots visible (n = 10). *LDB1(RNAi)* and *SSDP2 (RNAi)* regenerates have pointed blastemas with zero or one eyespot (6/6 and 9/10, respectively). D). *in situ* hybridization to mark the broadly expressed transcript *ChAT* (*choline acetyltransferase* (Nishimura et al., 2010);) in animals after RNAi, head amputation, and 6 days of regeneration. *LDB1(RNAi)* and *SSDP2(RNAi)* animals have smaller brains which are fused at the midline. E) Quantification of animals from a repetition of the experiment in (D) showing significantly smaller brains after *LDB1*(RNAi) and *SSDP2*(RNAi). (n = 5–9; Kruskal-Wallis with Dunn's correction for multiple comparisons.)

P is an adjusted value, * indicates $P \leq 0.05$ and ** indicates $P \leq 0.005$. Mean and SD are shown. Scale = 500 μm.

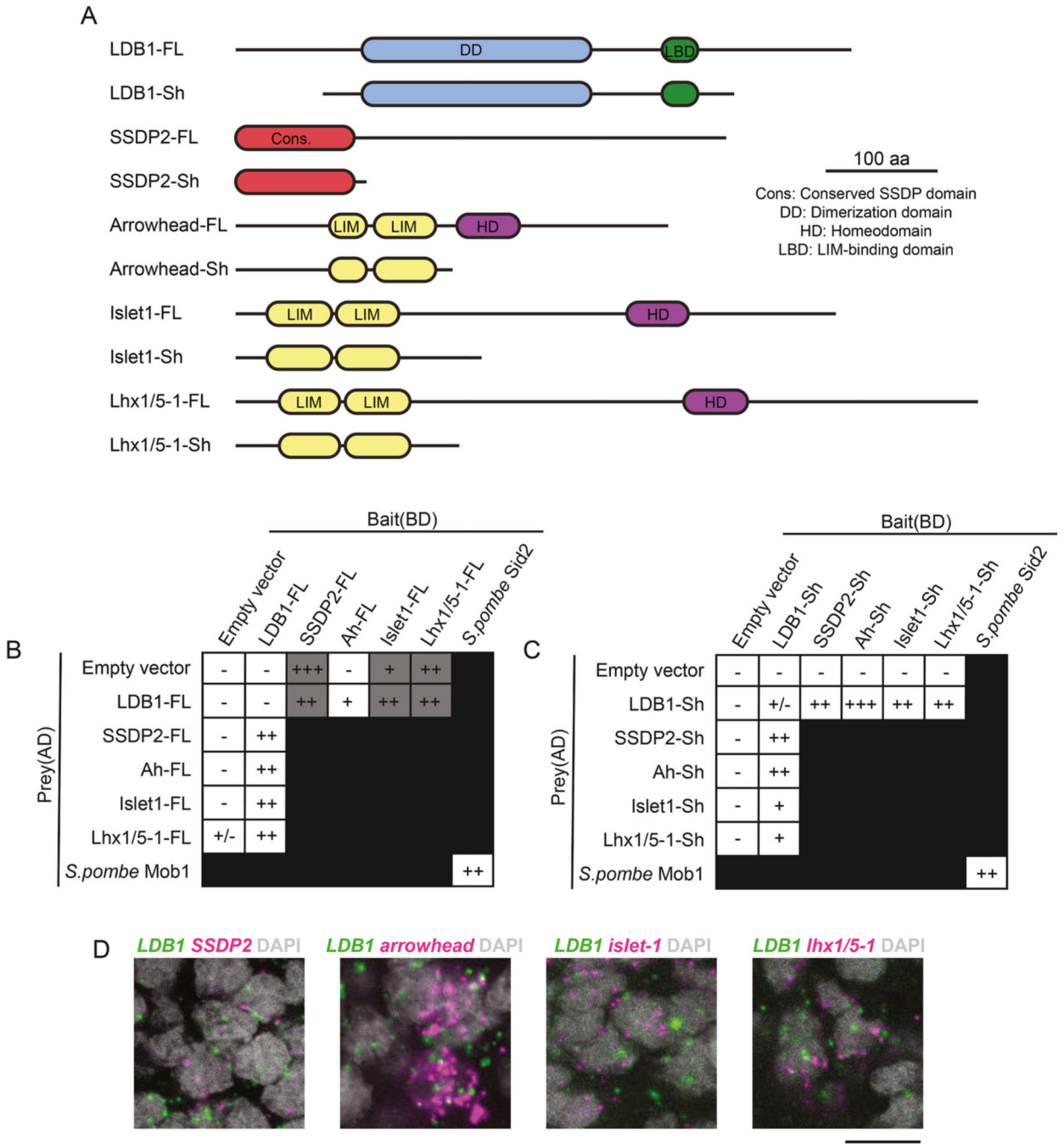

Fig. 2. Planarian LDB1 interacts with SSDP2, as well as the LIM domains of Arrowhead, Islet, and Lhx1/5–1.

A) Diagram showing domain architecture for LDB1, SSDP2, Arrowhead, Islet, and Lhx1/5–1. "FL" indicates full length protein and "Sh" indicates a shorter truncation used in subsequent analyses. The color scheme used is the same as in Fig. 1A. B) Yeast two-hybrid results showing the interaction of full-length LDB1 with full-length SSDP2, Arrowhead, Islet, and Lhx1/5–1. Full-length Ssdp2, Islet, and Lhx1/5–1 exhibited transactivation when used as the Bait (dark grey), so these pairings were not used for the final assessment. Full length planarian LDB1 did not show interaction with itself, despite

known homodimerization in other models. (- indicates no interaction; ± indicates weak growth; +, ++, or +++ indicates growth on restrictive medium). C) Yeast two-hybrid results showing that the core domains of LDB1 (LDB1-Sh) interact with the conserved domain of SSDP1 and the LIM domains of Arrowhead, Islet1, and Lhx1/5–1. In this experiment, we did note a weak self-interaction between the core domains of LDB1, which could support some dimerization of the protein. *S. pombe* Mob1 and Sid2 were used as controls (Balasubramanian et al., 1998; Hou et al., 2004). Cell growth for B and C is shown in Supp. Figs. 1A–B. D) Double FISH showing that *LDB1* is coexpressed with *SSDP2*, *arrowhead*, *islet1*, and *lhx1/5–1*. Scale = 10 μm.

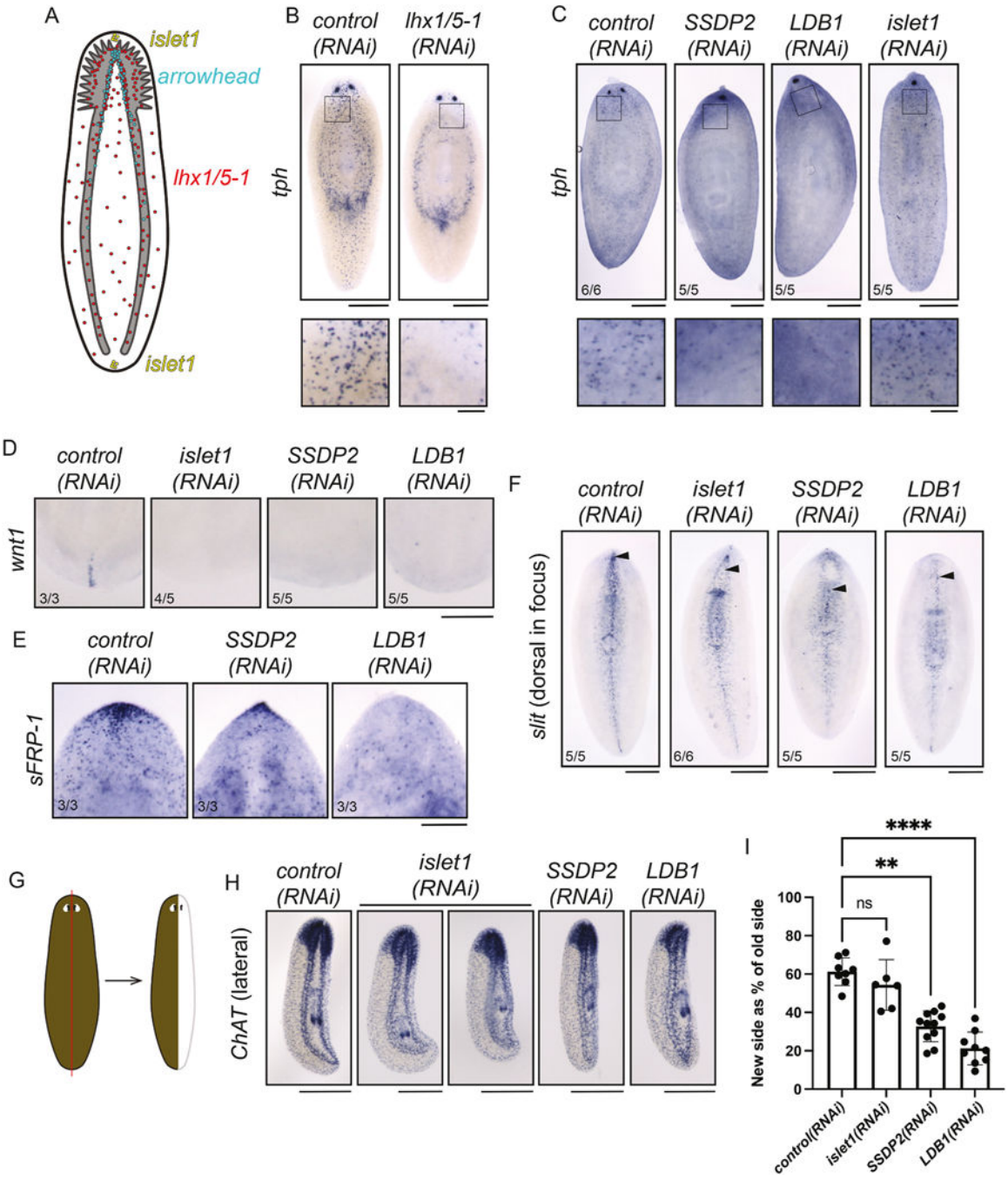

Fig. 3. *SSDP2(RNAi)* and *LDB1(RNAi)* phenotypes indicate functional overlap with Islet1 and Lhx1/5–1.

A) Diagram depicting published expression patterns of planarian LIM-HD-encoding genes *islet1* (Hayashi et al., 2011; Marz et al., 2013), *arrowhead* (Roberts-Galbraith et al., 2016), and *lhx1/5–1* (Currie and Pearson, 2013). B) *control(RNAi)* and *lhx1/5–1(RNAi)* animals underwent *in situ* hybridization with *TPH* (*tryptophan hydroxylase* (Nishimura et al., 2007);) 6 days after head amputation. Fewer peripheral *TPH*$^{+}$ neurons are seen after *lhx1/5–1(RNAi)* (see inset at bottom), as seen in a prior study (Currie and Pearson, 2013). C) control (RNAi), *SSDP2(RNAi), LDB1(RNAi),* and *islet1(RNAi)* animals stained for

TPH^{+} via *in situ* hybridization 6 days after head amputation. Fused eyespots are visible after *SSDP2(RNAi), LDB1(RNAi),* or *islet1(RNAi).* Decreased peripheral *TPH*$^{+}$ puncta were noted after knockdown of *SSDP2* or *LDB1,* but not *islet1* (see insets). D) *control (RNAi)*, *islet1(RNAi)*, *SSDP2(RNAi)* and *LDB1(RNAi)* animals underwent tail amputation, 6 days of regeneration, and *in situ* hybridization with the *Wnt1* probe (Adell et al., 2009; Petersen and Reddien, 2008). Only posterior ends are shown. E) *control(RNAi)*, *islet1(RNAi)*, *SSDP2(RNAi)* and *LDB1(RNAi)* animals underwent head amputation, 7 days of regeneration, and *in situ* hybridization with the *sFRP-1* probe (Gurley et al., 2008; Petersen and Reddien, 2008). Only anterior ends are shown. F) *control(RNAi)*, *islet1(RNAi)*, *SSDP2(RNAi)* and *LDB1(RNAi)* animals underwent head amputation, 6 days of regeneration, and *in situ* hybridization with the *slit1* probe (Cebrià et al., 2007). Animals were imaged with the dorsal side facing up; arrowheads indicate the anterior-most dorsal *slit* signal. G) Diagrams of the amputation plane used for experiments in (H). H) *control(RNAi)*, *islet1(RNAi)*, *SSDP2(RNAi)* and *LDB1(RNAi)* animals underwent sagittal amputation, 9 days of regeneration, and *in situ* hybridization with the *ChAT* probe (Nishimura et al., 2010). Animals are shown with the regenerating side to the right. I) We measured the area of both the newly regenerated brain lobe (right) and the existing brain lobe (left) and created a ratio for each animal in (H). *SSDP2(RNAi)* and *LDB1(RNAi)* animals regenerated significantly less new brain tissue than *control(RNAi)* animals. (n = 6–11; Kruskal-Wallis with Dunn's correction for multiple comparisons. P is an adjusted value, ** indicates $P \leq 0.005$ and **** indicates $P \leq 0.0001$). Mean and SD are shown. Scale = 500 μm (B, C, F, H), 100 μm (B, C insets), 200 μm (D, E).

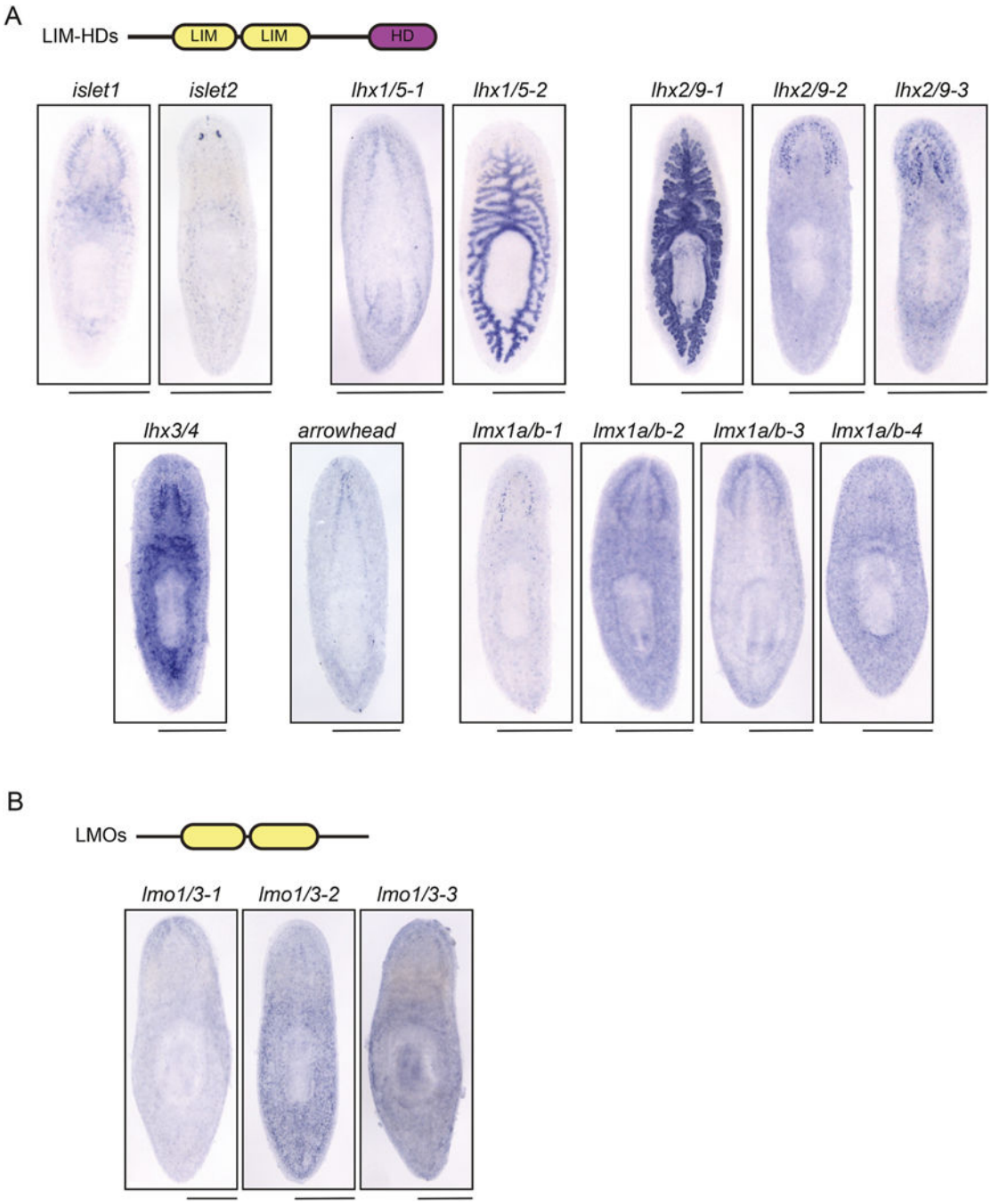

Fig. 4. Expression of planarian LIM-homeodomain and LIM-only-encoding genes.

A) Domain architecture of a typical LIM-homeodomain (LIM-HD) protein. 13 planarian genes encode LIM-HD proteins. Expression of these genes is shown in untreated planarians and genes are grouped by family. B) LIM-only (LMO) proteins have a typical domain architecture with two LIM domains each. 3 planarian genes encode LMO proteins. *in situ* hybridization for each LMO gene is shown. Scale = 500 μm.

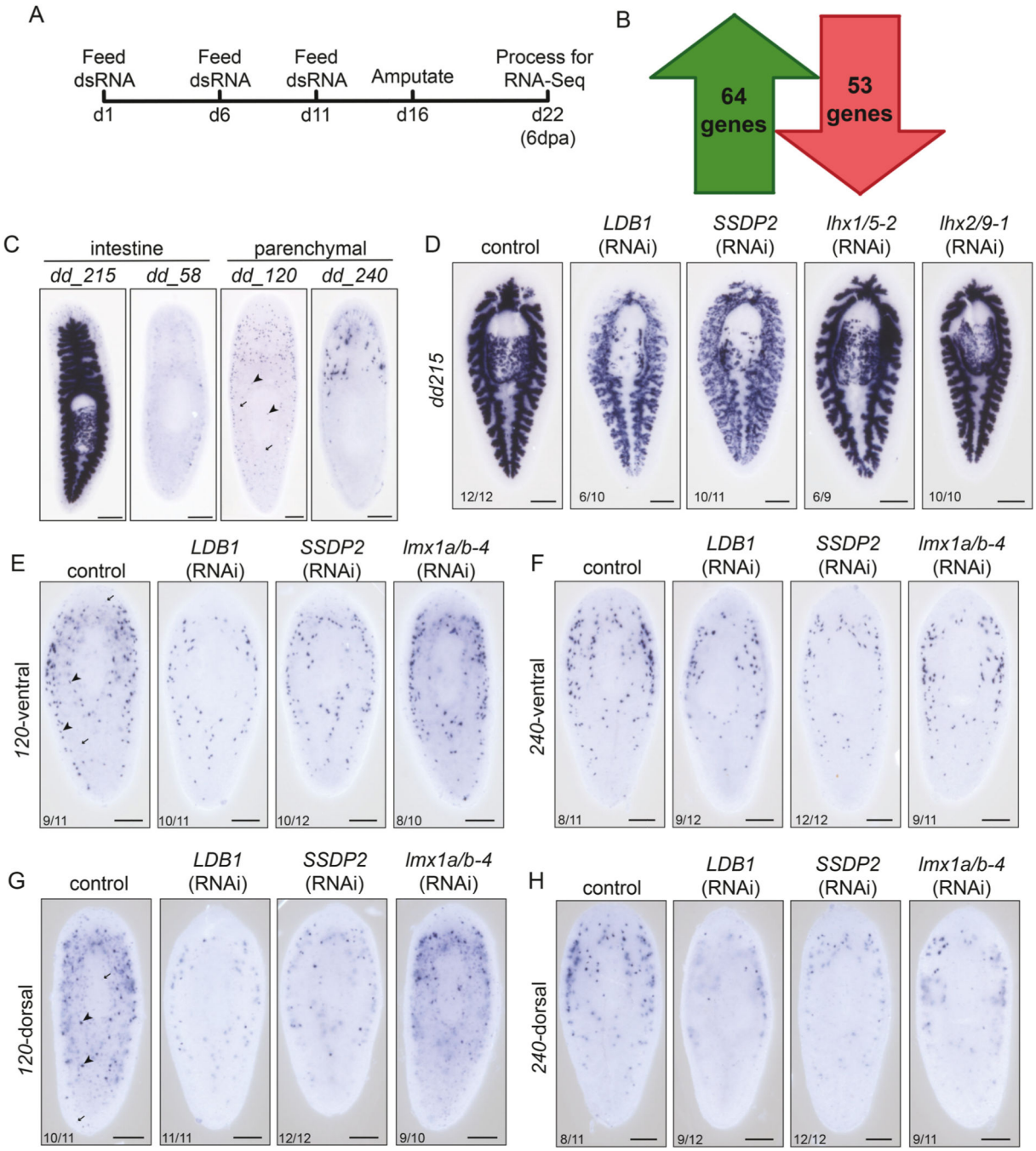

Fig. 5. Identification of genes differentially expressed after *SSDP2(RNAi)*.

A) RNAi paradigm used for bulk RNA-seq experiments. Animals underwent head amputation and 6 days of regeneration. B) We identified 64 genes that were upregulated ≥1.5x with a P value < 0.05 after false discovery rate correction. We also identified 53 genes that were downregulated ≥1.5x with a P value < 0.05 after false discovery rate correction. C) *In situ* hybridization showing normal expression of four genes significantly downregulated after *SSDP2(RNAi)*. Two parenchymal- and two intestine-enriched genes are shown. D) One transcript downregulated after *SSDP2(RNAi)* in our RNA-Seq data is *dd_215*. Using *in situ*

hybridization, we show that *dd_215* is absent from the blastema and is downregulated in both the existing intestine and pharynx after either *LDB1(RNAi)* or *SSDP2(RNAi)*, but not after knockdown of the gut-enriched LIM-HD-encoding genes *lhx1/5–2* or *lhx2/9–1*. E-H) *dd_120* and *dd_240* are decreased in expression after either *LDB1(RNAi)* or *SSDP2(RNAi)*, but not after knockdown of the parenchymal-enriched *lmx1a/b-4*. Ventral (E–F) and dorsal (G–H) views of animals are shown. For *dd_120*, we noted expression in two distinct cell types with strong (arrowhead) and weak (arrow) expression. Cells with weak expression are nearly absent after *LDB1(RNAi)* or *SSDP2(RNAi).* Animals are 6 days post-head amputation and both ventral (top) and dorsal (bottom) views are shown. Scale = 200 μm.